Neurosci Bull June 1, 2014, 30(3): 477–489. http://www.neurosci.cn
DOI: 10.1007/s12264-013-1432-x

·Original Article·

Grey-matter volume as a potential feature for the classification of Alzheimer's disease and mild cognitive impairment: an exploratory study

Yane Guo[1], Zengqiang Zhang[1,2], Bo Zhou[1], Pan Wang[1], Hongxiang Yao[3], Minshao Yuan[4], Ningyu An[3], Haitao Dai[2], Luning Wang[1], Xi Zhang[1], Yong Liu[5,6]

[1]*Department of Neurology, Institute of Geriatrics and Gerontology, Chinese PLA General Hospital, Beijing 100853, China*

[2]*Hainan Branch of Chinese PLA General Hospital, Sanya 572014, China*

[3]*Department of Radiology, Chinese PLA General Hospital, Beijing 100853, China*

[4]*Department of Neurology, the People's Hospital of Jimo, Qingdao 266200, China*

[5]*Brainnetome Center, Institute of Automation, Chinese Academy of Sciences, Beijing 100190, China*

[6]*National Laboratory of Pattern Recognition, Institute of Automation, Chinese Academy of Sciences, Beijing 100190, China*

Corresponding authors: Xi Zhang and Yong Liu. E-mail: zhangxi@301hospital.com.cn, yliu@nlpr.ia.ac.cn

ABSTRACT

Specific patterns of brain atrophy may be helpful in the diagnosis of Alzheimer's disease (AD). In the present study, we set out to evaluate the utility of grey-matter volume in the classification of AD and amnestic mild cognitive impairment (aMCI) compared to normal control (NC) individuals. Voxel-based morphometric analyses were performed on structural MRIs from 35 AD patients, 27 aMCI patients, and 27 NC participants. A two-sample two-tailed *t*-test was computed between the NC and AD groups to create a map of abnormal grey matter in AD. The brain areas with significant differences were extracted as regions of interest (ROIs), and the grey-matter volumes in the ROIs of the aMCI patients were included to evaluate the patterns of change across different disease severities. Next, correlation analyses between the grey-matter volumes in the ROIs and all clinical variables were performed in aMCI and AD patients to determine whether they varied with disease progression. The results revealed significantly decreased grey matter in the bilateral hippocampus/parahippocampus, the bilateral superior/middle temporal gyri, and the right precuneus in AD patients. The grey-matter volumes were positively correlated with clinical variables. Finally, we performed exploratory linear discriminative analyses to assess the classifying capacity of grey-matter volumes in the bilateral hippocampus and parahippocampus among AD, aMCI, and NC. Leave-one-out cross-validation analyses demonstrated that grey-matter volumes in hippocampus and parahippocampus accurately distinguished AD from NC. These findings indicate that grey-matter volumes are useful in the classification of AD.

Keywords: Alzheimer's disease; mild cognitive impairment; voxel-based morphometry; grey matter volume; classification

INTRODUCTION

Alzheimer's disease (AD) is the most common form of dementia in the elderly. AD is a neurodegenerative disorder pathologically characterized by the presence of amyloid deposits and neurofibrillary tangles[1]. The manifestations are progressive impairment of cognitive function and behavior. Currently, there is no effective treatment for this disease. Mild cognitive impairment (MCI) is a syndrome that

involves cognitive impairments greater than expected based on an individual's age and educational level but not severe enough to interfere with daily activities[2, 3]. Amnestic MCI (aMCI), a subtype of MCI, is characterized by mild memory impairments and clinically it frequently progresses into AD within a few years. Pathologically, aMCI is a prodromal stage of AD in the majority of cases observed at autopsy[4-7].

Currently, the diagnoses of AD and MCI are based on clinical presentation and psychological tests. However, the diagnosis of AD has lower sensitivity (~70%) and specificity (<70%) than the gold-standard neuropathological diagnosis[8]. Therefore, numerous studies have been designed to search for biomarkers of AD and MCI[9, 10], including cerebrospinal fluid (CSF) Aβ and total tau, and some imaging measures based on positron emission tomography and magnetic resonance imaging (MRI)[9, 11]. In addition, a recent cross-sectional study based on the Alzheimer's Disease Neuroimaging Initiative dataset has demonstrated that grey-matter atrophy reflects clinically-defined disease stages better than CSF biomarkers (such as Aβ and total tau)[12].

The evolution of patterns of grey-matter atrophy can be traced with the voxel-based morphometric (VBM) method; this method is hypothesis-free, rapid, sensitive in terms of localizing small-scale regional differences in grey matter, and easy to implement[13]. It has been widely applied to the study of regional grey-matter alterations in various disorders[14-21]. The medial temporal lobe (including the hippocampus and parahippocampus) most consistently exhibits decreased grey-matter volume in AD and MCI[12, 16, 17, 22-30]. Moreover, changes in grey-matter volumes in the entorhinal area[24], medial temporal lobe[22], hippocampus[31], and entorhinal area including the hippocampus and amygdala[25] have been reported to be candidate features of AD compared with normal controls (NCs). Nevertheless, heterogeneous grey-matter atrophy patterns have been reported in AD and MCI[32, 33], and few studies have investigated the ability of grey-matter volumes to discriminate between AD, MCI, and NC.

In this study, we focused on three questions: (1) where and how grey matter volumes are altered in Chinese AD patients compared to NCs; (2) whether aMCI patients exhibit AD-like changes in the identified regions; and (3) whether grey matter volumes discriminate AD/aMCI patients from NCs.

PARTICIPANTS AND METHODS

Portions of the fMRI data in the present study have been used in our previous studies of regional homogeneity[34], amygdala connectivity[35], and thalamic connectivity[36] during the resting state. To maintain the scientific integrity of the present study, we provide a short description of the data collection and data preprocessing.

Ethics Statement

This study was approved by the Medical Ethics Committee of the PLA General Hospital and conducted according to the principles of the Declaration of Helsinki. Before selection for the study, all potential participants underwent general physical, psychological, and laboratory examinations. All were informed about the aims of the study, and written informed consent was given by all participants or their legal guardians. Anyone who chose not to participate was still eligible for treatment (if applicable) and was not disadvantaged in any way by not participating in the study.

Participants

The participants were outpatients of the Chinese PLA General Hospital or were recruited by advertisement (http://www.301ad.com.cn), and all were evaluated at the Chinese PLA General Hospital, Beijing, China. They were all right-handed and underwent a neuropsychological test battery that comprised the Mini-Mental State Examination (MMSE), the Auditory Verbal Learning Test (AVLT), the Geriatric Depression Scale[37], Clinical Dementia Rating (CDR)[38] and the Activities of Daily Living scale (ADL). In brief, the AVLT consisted of one learning trial in which a list of 10 Chinese double-character words was read, and the participant was asked to immediately recall as many items as possible. Next, the trial was repeated twice, and the immediate recall score taken as the mean accurate recall over the three trials. After a 5-min delay, each participant was asked to recall the words from the initial list (AVLT delayed-recall). The participants were then asked to identify the 10 studied words from a word set that also included 10 novel words (AVLT recognition). The demographic and neuropsychological scores of the participants are listed in Table 1.

The criteria for diagnosing aMCI were as stated in Petersen *et al.*[3]: (1) memory complaints that persisted for at least six months; (2) CDR = 0.5; (3) intact functional status and ADL <26; and (4) no dementia according to the criteria

Table 1. Demographic, clinical, and neuropsychological data for the normal controls (NCs), amnestic mild cognitive impairment (aMCI) and Alzheimer's disease (AD) patients.

	NC (*n*=27)	aMCI (*n*=27)	AD (*n*=35)	*P* value
Gender (Male/Female)	16/11	13/14	12/23	0.143
Age (years)	69.2±6.5	73.8±7.8	72.4±8.5	0.09
MMSE	28.9±1.0	26.8±1.8[a]	19.7±4.1[a,b]	<0.001
CDR	0	0.5	1.3±0.5[a,b]	<0.001
AVLT-Immediate Recall[c]	5.9±1.1	4.6±1.5	2.6±1.6[a,b]	<0.001
AVLT-Delay Recall[c]	5.8±2.0	3.1±2.0[a]	0.6±1.2[a,b]	<0.001

The χ^2 test was used for gender comparisons; one-way ANOVA with Bonferroni *post hoc* tests was used for the age and neuropsychological test comparisons. [a]Significant compared to NC. [b]Significant compared to aMCI. [c]Three AD patients refused to continue this test. AVLT, auditory verbal learning test; CDR, clinical dementia rating; MMSE, mini-mental state examination.

of the International Classification of Diseases, 10th Revision (ICD-10). The participating AD patients fulfilled the following inclusion criteria: (1) AD diagnosis based on the ICD-10 criteria; (2) CDR = 1 or 2; (3) free of the use of nootropic drugs such as anticholinesterase inhibitors; and (4) capable of performing the neuropsychological tests and tolerating the MR scanning. The criteria for the NC participants comprised the following: (1) normal general physical status; (2) CDR = 0; and (3) free of memory complaints.

The exclusion criteria for all participants were as follows: (1) metabolic conditions such as hypothyroidism or vitamin B12 or folic acid deficiencies; (2) psychiatric disorders such as depression or schizophrenia; (3) brain infarction or hemorrhage as indicated by MR/CT imaging; and (4) Parkinsonian syndromes, epilepsy, or other nervous system diseases that can influence cognitive function. Moreover, any participant with a metallic foreign body, such as a cochlear implant or heart stent, and any participant with any contraindication for MR scanning was excluded.

Data Acquisition

Sagittal structural images with a resolution of 0.94 × 0.94 × 1.2 mm^3 were acquired using a three-dimensional magnetization-prepared rapid gradient echo with a 3.0 T GE MR system (GE Healthcare, Milwaukee, WI) using a standard head coil. The scanning parameters were as follows: repetition time, 2 000 ms; echo time, 2.6 ms; and flip angle, 9°. During the MRI scans, all participants were instructed to relax and move as little as possible. Tight but comfortable foam padding was used to reduce head motion, and earplugs were used to minimize scanner noise.

Data Preprocessing

Structural data were processed using Statistical Parametric Mapping software (SPM8, http://www.fil.ion.ucl.ac.uk/spm), and we implemented VBM analysis with the VBM8 toolbox (http://dbm.neuro.uni-jena.de/vbm.html) using the default parameters. Images were captured for grey-matter, white-matter, and CSF segments. The images were bias-corrected, tissue classified, and registered using linear (affine transform) and non-linear transformations (warping). Next, further analyses were performed on the grey-matter, white-matter, and CSF images, which were multiplied by the determinant of the Jacobian transform matrix for the non-linear component of the transformation to preserve the actual, local grey-matter and white-matter volumes (i.e., the modulated grey/white-matter volumes). Finally, the modulated grey-matter volumes were re-sliced to 2 × 2 × 2 mm^3 and smoothed with 6 mm at full width and half maximum Gaussian kernel[29].

Statistical Analysis

To avoid possible white-matter/CSF effects, we introduced the automated anatomical labeling (AAL) template from the MRIcron toolkit (http://www.mccauslandcenter.sc.edu/mricro/mricron/) as a mask. Two-sample two-tailed *t*-tests were performed between the NC and AD groups to create a map of abnormal grey matter. The threshold for the resultant *T*-value map was set at $P < 0.001$ [$T = 6.047$, df = (1, 60), family-wise error (FWE) corrected] for each voxel with cluster sizes of at least 40 voxels. Subsequently, the regions with significant differences were extracted as regions of interest (ROIs), and the grey-matter volumes in these identified regions from the aMCI patients were included to evaluate changes in grey-matter patterns across different levels of disease severity.

Statistical comparisons of the mean grey-matter volumes within each identified ROI between each pair of groups (NC *versus* aMCI, aMCI *versus* AD, and NC *versus*

AD) were performed with two-sample, two-tailed *t*-tests at a threshold P <0.05 (FDR-corrected based on the number of groups multiplied by the number of significant brain regions). Identical whole-brain voxel-wise analyses were performed between the NC and aMCI groups and the aMCI and AD groups.

Relationships between Grey-matter Volume and Clinical Assessment

To determine whether grey-matter volume reflects disease severity, Pearson correlation analyses of the grey-matter volumes of the identified regions and each of the clinical assessments (MMSE, AVLT immediate/delayed-recall and recognition scores) were performed for the aMCI, AD, and aMCI plus AD groups. Because these analyses were exploratory in nature, we used a statistical significance level of P <0.05 (uncorrected).

RESULTS

Group Differences in Grey-matter Volume

In AD patients, the regions with significantly decreased grey-matter volumes compared to NCs included the bilateral hippocampus/parahippocampus (Hip/Phip), the bilateral superior/middle temporal gyri (STG/MTG) and the right precuneus (Pcu) (Table 2 and Fig. 1). In addition, the grey-matter volumes in the identified regions were decreased in the aMCI patients relative to the NCs (P < 0.05, FDR-corrected) (Fig. 2). Furthermore, the grey-matter volumes in the bilateral Hip/Phip and bilateral STG/MTG were lower in the AD than in the aMCI patients (P <0.05, FDR-corrected) (Fig. 2).

Whole-brain voxel-wise analyses revealed no significant differences between the NC and aMCI groups or between the aMCI and AD groups at the threshold of P <0.05 (FWE-corrected). However, with a more relaxed threshold of P <0.001, cluster size >40 voxels (uncorrected), similar patterns of grey matter change were found in the aMCI and AD groups when compared to the NC group (Fig. S1).

Relationships between Grey-matter Volume and Clinical Variables

In the aMCI plus AD group, the grey-matter volumes of all identified regions exhibited significant correlations with the

Table 2. Regions with significantly reduced grey-matter volume in Alzheimer's disease (AD) patients compared to normal controls

Region	BA	Cluster size	*T* value	*Z*	MNI coordinates (x,y,z)
Hip/Phip.L	28/34	1434	11.27	8.22	-28 -12 -16
			8.13	6.65	-20 -22 -14
			7.60	6.34	-18 -38 -2
Hip/Phip.R	28/34	1391	10.12	7.69	26 -10 -16
			8.43	6.82	20 -36 0
			7.60	6.33	38 -30 -12
STG/MTG.L	21/22	649	7.86	6.49	-54 -36 -4
			6.40	5.56	-58 -10 -8
			6.25	5.47	-60 -18 -6
STG/MTG.R		278	6.89	5.89	60 -22 -6
			6.38	5.55	62 -38 6
			5.93	5.24	64 -30 -2
Pcu.R	7/31	118	6.37	5.55	12 -66 24
			6.26	5.47	10 -54 22

BA, Brodmann's area; Hip, hippocampus; L, left; MTG, middle temporal gyrus; Pcu, precuneus; Phip, parahippocampus; R, right; STG, superior temporal gyrus.

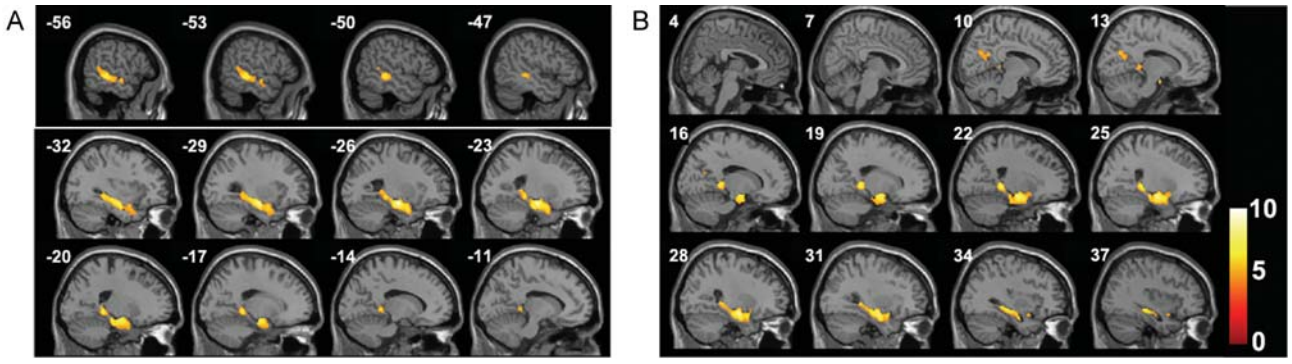

Fig. 1. Brain areas with greater grey-matter atrophy in AD patients compared to NC participants. A: left hemisphere; B: right hemisphere (*P* < 0.001, FWE-corrected, cluster size >40 voxels). Details of the regions are in Table 2.

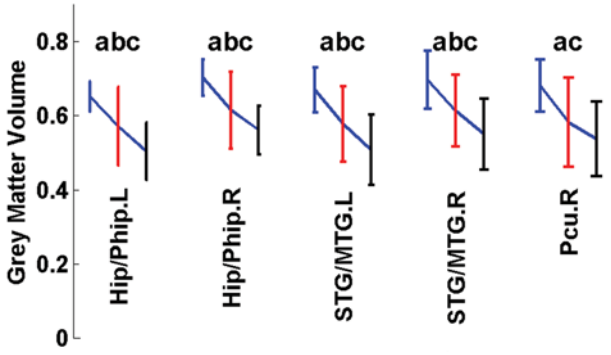

Fig. 2. Plots of the grey-matter volume in NC (blue), aMCI (red), and AD (black) participants in the indicated regions (*P* <0.05, FDR-corrected). Volumes significantly differed between the NC and aMCI groups (a), aMCI and AD groups (b), and NC and AD groups (c).

MMSE and AVLT delayed-recall scores (Table 3, Fig. 3 A, B); the grey-matter volumes of all identified regions except the right precuneus exhibited significant correlations with the new word recognition scores (*P* <0.05) (Table 3, Fig. 3D).

In the aMCI group, the grey-matter volumes of the bilateral Hip/Phip and the left STG/MTG showed significant correlations with the AVLT delayed-recall and new word recognition scores (Table 3, Fig. 3B, D). The grey-matter volumes of the right STG/MTG were significantly correlated with the AVLT immediate-recall scores (Table 3, Fig. 3C).

Exploratory Classification Analyses

The grey matter of the bilateral Hip/Phip showed the most severe atrophy in the AD group (Figs. 1 and 2), which is consistent with most previous studies[16, 17, 23, 24]. To evaluate the potential use of grey-matter volumes for diagnosis, the bilateral Hip/Phip in the AAL template were selected using the WFU_PickAtlas toolkit (www.ansir.wfubmc.edu)[39]. As different parts of the hippocampus play different roles in memory[40] and the head and tail are most severely impaired in AD[19, 41], we further divided each hippocampus and parahippocampus into four subregions: the head, parts 1 and 2 of the body, and the tail (Fig. S2). Thus 16 features for each participant were used in the discriminative and cross-validation analyses. Next, Fisher's linear discriminative method (see Appendix) and leave-one-out cross-validation analyses were performed to assess the utility of grey-matter volumes to classify patients[41-44]. We also randomly left 2 to 5 participants out and re-performed the cross-validation analyses to test the robustness of the classification. The results revealed ~82% accuracy in discriminating AD patients from NC participants (Table 4, Fig. 4A, Fig. S3). And ~58% of the cases were correctly classified when the same protocol was used to distinguish all three groups (Table 5, Fig. 4B, Fig. S4).

DISCUSSION

Grey-matter Atrophy in AD/aMCI

In the present study, the most marked atrophy of grey matter in AD was in the hippocampus and parahippocampus, regions that have been most consistently reported to exhibit significant reductions in grey matter in AD[16, 17, 22-29]. Previous histopathological studies have shown that the hippocampus and parahippocampus are the first regions to be affected by neurofibrillary tangles

Table 3. Correlations between grey-matter volumes and clinical variables in AD and aMCI

Region	Clinical Variance	AD & aMCI		aMCI		AD	
		CC	*P*	*CC*	*P*	*CC*	*P*
Hip/Phip.L	MMSE	0.337	0.007	0.066	0.745	0.184	0.289
	AVLT immediate recall	0.220	0.094	0.346	0.077	0.217	0.232
	AVLT delayed recall	0.583	<0.001	0.594	0.001	0.245	0.177
	New word recognition	0.311	0.017	0.504	0.007	0.032	0.863
Hip/Phip.R	MMSE	0.279	0.028	0.064	0.751	0.127	0.468
	AVLT immediate recall	0.096	0.472	0.272	0.170	0.006	0.973
	AVLT delayed recall	0.560	<0.001	0.618	0.001	0.186	0.308
	New word recognition	0.274	0.036	0.529	0.005	-0.012	0.946
STG/MTG.L	MMSE	0.350	0.005	0.069	0.733	0.212	0.221
	AVLT immediate recall	0.227	0.083	0.361	0.064	0.198	0.278
	AVLT delayed recall	0.422	0.001	0.517	0.006	-0.057	0.757
	New word recognition	0.377	0.003	0.628	<0.001	0.159	0.384
STG/MTG.R	MMSE	0.297	0.019	0.152	0.448	0.102	0.560
	AVLT immediate recall	0.145	0.272	0.405	0.036	0.058	0.751
	AVLT delayed recall	0.325	0.012	0.248	0.212	0.003	0.986
	New word recognition	0.313	0.016	0.216	0.278	0.169	0.355
Pcu.R	MMSE	0.270	0.034	0.165	0.411	0.213	0.218
	AVLT immediate recall	0.069	0.603	0.155	0.440	0.016	0.929
	AVLT delayed recall	0.342	0.008	0.288	0.145	0.170	0.353
	New word recognition	0.232	0.077	0.349	0.075	0.063	0.733

CC, correlation coefficient; Hip, hippocampus; L, left; MTG, middle temporal gyrus; Pcu, precuneus; Phip, parahippocampus; R, right; STG, superior temporal gyrus

Table 4. Summary of the results of exploratory classification of the NC and AD groups

		Group	Predict group		Total
			NC	AD	
Original	Classify count	NC	27	0	
		AD	2	33	
	Correct ratio (%)	NC	100	0	
		AD	5.7	94.3	96.7
Cross-validated [a]	Classify count	NC	23	4	
		AD	7	28	
	Correct ratio (%)	NC	85.2	14.8	
		AD	20	80	82.3

[a]Leave-one-out cross-validation.

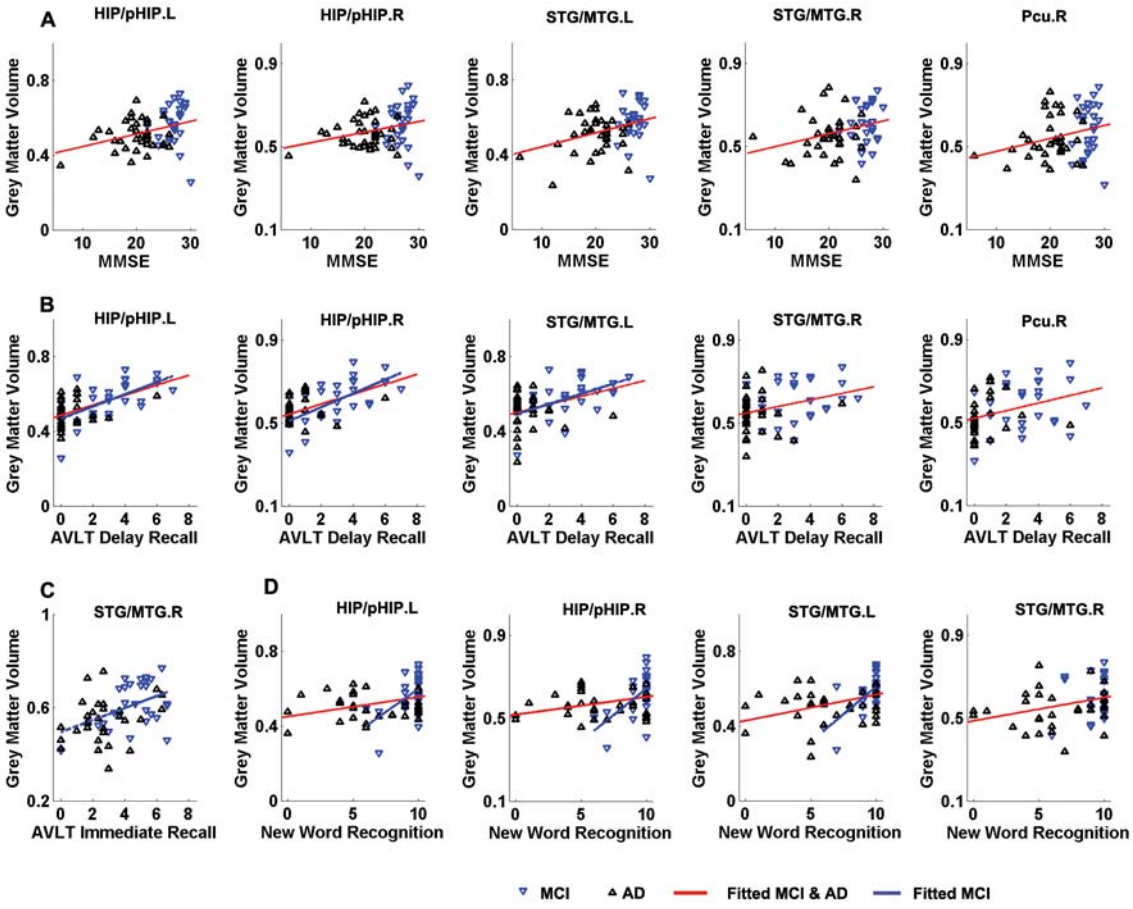

Fig. 3. Correlations between mean grey-matter volume in the indicated regions and neuropsychological test measures in aMCI, AD, and aMCI & AD patients (P <0.05). Details of the correlation coefficients and P-values are in Table 3.

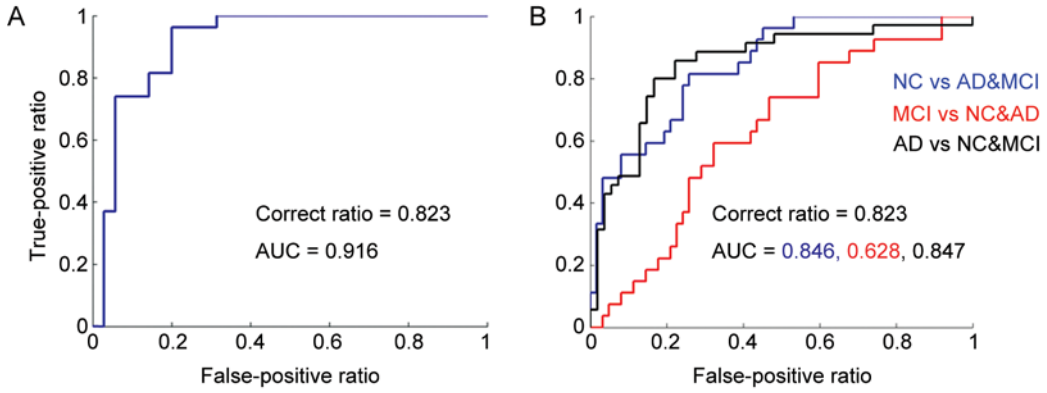

Fig. 4. A: ROC curves showing that linear discriminative and leave-one-out cross-validation analyses resulted in accurate discrimination of AD patients from NCs. B: ROC curves showing that linear discriminative and leave-one-out cross-validation analyses resulted in accurate classification of NC (blue), aMCI (red), and AD (black). Details of the correlation coefficients and P-values are in Tables 4–5. AUC, area under the curve; correct ratio, percentage of correctly-classified participants out of the total number of participants.

Table 5. Summary of the results of exploratory classification of the NC, aMCI, and AD groups

		Group	Prediction group			Total
			NC	aMCI	AD	
Original	Classify count	NC	22	5	0	
		MCI	2	18	7	
		AD	1	3	31	
	Correct ratio (%)	NC	81.5	18.5	0	
		MCI	7.4	66.7	25.9	
		AD	2.8	8.6	88.6	79.8
Cross-validated[a]	Classify count	NC	16	10	1	
		MCI	8	11	8	
		AD	3	7	25	
	Correct ratio (%)	NC	59.3	37.0	3.7	
		MCI	29.6	40.7	29.6	
		AD	8.6	20	71.4	58.4

[a] Here, we provide the results of the leave-one-out cross-validation.

and amyloid plaques, and also exhibit the greatest loss of neurons in AD[45, 46]. Furthermore, the positive correlations between grey-matter volumes and clinical variables (Fig. 3) provided evidence that grey-matter atrophy in the Hip/Phip may be helpful in AD diagnosis, and this was subsequently confirmed with the discriminative analyses (Tables 4 and 5, Fig. 4). Providing further support for the present results, significantly decreased grey-matter volumes in the STG/MTG and precuneus in AD have also been widely reported[16, 17, 23, 26-28]. Atrophy of grey matter in these regions also supports previous findings that the initial pathological changes in AD occur in the medial temporal lobe and then spread to the other temporal lobe regions[45, 47].

The major manifestation of aMCI is memory impairment, and because aMCI has a high risk of progression to AD, it is considered a prodromal stage[2, 4]. In this study, the medial locations of the identified regions of grey matter in the aMCI patients partially reflected this transitional stage (Fig. 2, Fig. S1). In addition, the significant alterations in the bilateral Hip/Phip and STG/MTG between each pair of the three groups suggested that intense pathological changes occur in these regions throughout the development of AD.

Correlation of Grey-matter Volumes with Clinical Variables

Interestingly, grey-matter volumes in the identified regions were significantly correlated with the neuropsychological test scores (Table 3, Fig. 3). The MMSE is a brief screening tool that quantitatively assesses the severity of cognitive impairment and reflects cognitive changes that occur during the progression of AD[48]. The correlations between MMSE and grey-matter volumes indicated that abnormal grey-matter atrophy might represent the severity of disease and could be used to distinguish patients from healthy individuals. The AVLT immediate-recall test consists of a list of learning tasks and indicates verbal short-term memory, whereas the AVLT delayed-recall test measures episodic memory. The positive correlations between grey-matter volumes in all of the identified regions and AVLT recall scores reflected decreases in episodic memory that are associated with brain atrophy in these regions in the patient groups. In addition, the strongest relationship was between the bilateral Hip/Phip and the AVLT delayed-recall test, indicating the primary role of the Hip/Phip in episodic memory. Notably, we evaluated the relationships between grey-matter volumes and clinical variables in the aMCI plus AD group to investigate the relationship between the severity of grey-matter atrophy and cognitive ability, since aMCI is an early symptomatic stage of AD[7, 49, 50]. However, the correlations between grey-matter volumes and clinical variables in some of the identified regions in the aMCI or

AD group were weak or absent (Table 3, Fig. 3). Therefore, the correlations may only be indicative of the general relationship between grey-matter atrophy and cognitive performance in the AD and aMCI patients and may have been influenced by group effects because not all aMCI patients convert to AD.

Is Grey-matter Atrophy Useful for Distinguishing between AD and MCI?

From a clinical perspective, the ultimate goal of the present study was to find biomarkers capable of discriminating patients from NCs. Although the pathophysiological processes of AD far precede the diagnosis[50-52], here we found that grey-matter volumes have the potential to be used to identify AD (>82% of cases were correctly classified in the cross-validation tests) (Table 4, Fig. 4A, Fig. S3), consistent with many previous studies[25, 31, 53]. However, the same analysis protocol did not perform well (~58% of cases were correctly identified in the cross-validation tests) when the aMCI patients were included (Table 5, Fig. 4B, Fig. S4). Several reasons may account for this decrease: whether and when aMCI patients convert to AD are uncertain[4, 7, 54-56]; the AD patients in the present study were at a relatively mild stage (25 patients CDR = 1; 10 patients CDR = 2), which indicated an overlap in grey-matter atrophy between the AD and aMCI groups (Fig. 2); and the pathological changes that underlie cognitive loss in patients with AD might emerge 10–20 years before symptoms of dementia[57], implying that some of the NCs might have been in the preclinical stage of AD. Therefore, combinations of biomarkers and large samples are needed in the future.

Methodological Issues and Discussion of Comparisons

The patterns of grey-matter atrophy observed in the present study are in accord with previous findings; however, our results of whole brain voxel-wise analyses did not reveal significant differences between the NC and aMCI groups or between the aMCI and AD groups at the threshold of P <0.05 (FWE-corrected). Nevertheless, the atrophy patterns of aMCI and AD were similar when a less strict threshold was used [P <0.001, cluster size >40 voxels (uncorrected)(Fig. S1), which indicated that aMCI may be a prodromal stage of AD and that more severe symptoms are accompanied by more severe grey-matter atrophy (Fig. S1). In contrast, it should also be noted that there was a trend toward statistical significance in age and gender among the NC, aMCI, and AD participants. Further analyses revealed similar patterns of grey-matter atrophy in AD regardless of whether age and gender were controlled for (Table S1, Fig. S5). Furthermore, we still do not have consistent criteria regarding the parcellation of the bilateral hippocampus and parahippocampus[58, 59]; thus, average parcellation of brain regions cannot provide detailed functional information about the subregions. In addition, previous studies have suggested that direct imaging of the pathologic substrates would require a validation process based on longitudinal studies to test their usefulness as markers of AD/MCI[50, 51, 60]. Hence, longitudinal datasets with large sample sizes and a detailed brain atlas are required to generate more valuable biomarkers that are expected to form a more effective computer-aided diagnostic tool for AD/MCI in the future.

Another issue is that, despite the advantages of VBM, this technique has some drawbacks. During image preprocessing, there may be biases in the segmentation steps in regions with poor tissue contrast that may be particularly evident in the aging brain, especially in AD/MCI brains. In addition, there may be registration errors in the spatial normalization step. Moreover, image smoothing with a Gaussian filter kernel (kernel = 6 mm in the present study) is necessary to make the data more normally distributed for statistical analysis; this process may lead to problems in localizing between-group volumetric differences in some of the smaller brain areas[61-63].

SUPPLEMENTAL DATA

Supplemental data include five figures and one table and can be found online at http://www.neurosci.cn/epData.asp?id=181.

ACKNOWLEDGEMENTS

This work was partially supported by the National Natural Science Foundation of China (60831004 and 81270020), the CASIA Fund for Young Scientists with Lu-Jia-Xi award, the Specific Healthcare Research Projects (13BJZ50), the Clinical Sciences Fund of the Chinese PLA General Hospital (2013FC-TSYS-1006) and the Science Technological Innovation Nursery Fund of the Chinese PLA General Hospital (13KMM19), China.

APPENDIX. Fisher's Linear Discriminant Analysis (FLDA) for Multiple Classes[44, 64]

The primary goal of FLDA is to discriminate samples of different groups by maximizing the ratio of between-class separability to within-class variability. Suppose that we have K classes C_k, and x is the feature; we need to find a projection w and transform the feature to y. In the simplest case, the model is linear in the input variables and therefore takes the form $y(x) = w^T x + w_0$ so that y is a real number. According to Bayes' theorem, we can adopt a generative approach in which we model the class-conditional densities given by $p(x|C_K)$, together with the prior probabilities $p(C_k)$ for the classes. We can then compute the required posterior probabilities using $p(C_k|x) = \frac{p(x|C_k)p(C_k)}{p(x)}$.

Theoretically, the within-class covariance matrix is

$$S_w = \sum_{k=1}^{K} \sum_{n \in C_k} (y_n - u_k)(y_n - u_k)^T, \text{where} \quad u_k = \frac{1}{N_k} \sum_{n \in C_k} y_n$$

N_k is the number of samples in class C_k. The between-class covariance matrix can be defined by

$$S_B = \sum_{k=1}^{K} N_k (u_k - u)(u_k - u)^T, \text{where } u = \frac{1}{N} \sum_{k=1}^{k} N_k u_k$$

The main objective of FLDA is to find a projection direction w that maximizes the objective function as

$$J(w) = \frac{w^T S_B w}{w^T S_w w}$$

Theoretically, there are many methods with which we could compute the projective function w; here, we employed a probabilistic view of classification and computed the linear decision boundaries based on simple assumptions about the distribution of the data.

$$a_k(x) = w_k^T x + w_{k0}$$

where

$$w_k = \sum^{-1} u_k, \quad w_{k0} = -\frac{1}{2} u_k^T \sum^{-1} u_k + lnP(C_k),$$

and $P(C_k)$ is the probability for y belonging to class K.

Then, we have

$$p(C_k|x) = \frac{p(x|C_k)p(C_k)}{\sum_j p(x|C_j)p(C_j)} = \frac{\exp(a_k)}{\sum_j \exp(a_j)}$$

which is known as the normalized exponential and can be regarded as a multiclass generalization of the logistic sigmoid. If $p(C_j|x) >> p(C_i|x)$, i=1,2..K, $i \neq j$, then we can identify x to the jth class.

Received date: 2013-07-20; Accepted date: 2013-10-28

REFERENCES

[1] Hardy J, Selkoe DJ. The amyloid hypothesis of Alzheimer's disease: progress and problems on the road to therapeutics. Science 2002, 297: 353–356.

[2] Gauthier S, Reisberg B, Zaudig M, Petersen RC, Ritchie K, Broich K, *et al.* Mild cognitive impairment. Lancet 2006, 367: 1262–1270.

[3] Petersen RC, Smith GE, Waring SC, Ivnik RJ, Tangalos EG, Kokmen E. Mild cognitive impairment: clinical characterization and outcome. Arch Neurol 1999, 56: 303–308.

[4] Petersen RC, Parisi JE, Dickson DW, Johnson KA, Knopman DS, Boeve BF, *et al.* Neuropathologic features of amnestic mild cognitive impairment. Arch Neurol 2006, 63: 665–672.

[5] Schneider JA, Arvanitakis Z, Leurgans SE, Bennett DA. The neuropathology of probable Alzheimer disease and mild cognitive impairment. Ann Neurol 2009, 66: 200–208.

[6] Ward A, Arrighi HM, Michels S, Cedarbaum JM. Mild cognitive impairment: disparity of incidence and prevalence estimates. Alzheimers Dement 2012, 8: 14–21.

[7] Albert MS, DeKosky ST, Dickson D, Dubois B, Feldman HH, Fox NC, *et al.* The diagnosis of mild cognitive impairment due to Alzheimer's disease: recommendations from the National Institute on Aging-Alzheimer's Association workgroups on diagnostic guidelines for Alzheimer's disease. Alzheimers Dement 2011, 7: 270–279.

[8] Knopman DS, DeKosky ST, Cummings JL, Chui H, Corey-Bloom J, Relkin N, *et al.* Practice parameter: diagnosis of dementia (an evidence-based review). Report of the Quality Standards Subcommittee of the American Academy of Neurology. Neurology 2001, 56: 1143–1153.

[9] Hampel H, Burger K, Teipel SJ, Bokde AL, Zetterberg H, Blennow K. Core candidate neurochemical and imaging biomarkers of Alzheimer's disease. Alzheimers Dement 2008, 4: 38–48.

[10] Xu XH, Huang Y, Wang G, Chen SD. Metabolomics: a novel approach to identify potential diagnostic biomarkers and pathogenesis in Alzheimer's disease. Neurosci Bull 2012, 28: 641–648.

[11] Jack CR Jr, Lowe VJ, Senjem ML, Weigand SD, Kemp BJ, Shiung MM, *et al.* 11C PiB and structural MRI provide complementary information in imaging of Alzheimer's disease and amnestic mild cognitive impairment. Brain 2008, 131: 665–680.

[12] Vemuri P, Wiste HJ, Weigand SD, Shaw LM, Trojanowski JQ,

Weiner MW*, et al.* MRI and CSF biomarkers in normal, MCI, and AD subjects: diagnostic discrimination and cognitive correlations. Neurology 2009, 73: 287–293.

[13] Ashburner J, Friston KJ. Voxel-based morphometry--the methods. Neuroimage 2000, 11: 805–821.

[14] Baron JC, Chetelat G, Desgranges B, Perchey G, Landeau B, de la Sayette V*, et al. In vivo* mapping of gray matter loss with voxel-based morphometry in mild Alzheimer's disease. Neuroimage 2001, 14: 298–309.

[15] Frisoni GB, Testa C, Zorzan A, Sabattoli F, Beltramello A, Soininen H*, et al.* Detection of grey matter loss in mild Alzheimer's disease with voxel based morphometry. J Neurol Neurosurg Psychiatry 2002, 73: 657–664.

[16] Karas GB, Burton EJ, Rombouts SA, van Schijndel RA, O'Brien JT, Scheltens P*, et al.* A comprehensive study of gray matter loss in patients with Alzheimer's disease using optimized voxel-based morphometry. Neuroimage 2003, 18: 895–907.

[17] Whitwell JL, Przybelski SA, Weigand SD, Knopman DS, Boeve BF, Petersen RC*, et al.* 3D maps from multiple MRI illustrate changing atrophy patterns as subjects progress from mild cognitive impairment to Alzheimer's disease. Brain 2007, 130: 1777–1786.

[18] Risacher SL, Saykin AJ, West JD, Shen L, Firpi HA, McDonald BC*, et al.* Baseline MRI predictors of conversion from MCI to probable AD in the ADNI cohort. Curr Alzheimer Res 2009, 6: 347–361.

[19] Shi F, Liu B, Zhou Y, Yu C, Jiang T. Hippocampal volume and asymmetry in mild cognitive impairment and Alzheimer's disease: Meta-analyses of MRI studies. Hippocampus 2009, 19: 1055–1064.

[20] Kostic VS, Agosta F, Petrovic I, Galantucci S, Spica V, Jecmenica-Lukic M*, et al.* Regional patterns of brain tissue loss associated with depression in Parkinson disease. Neurology 2010, 75: 857–863.

[21] Tan L, Fan Q, You C, Wang J, Dong Z, Wang X*, et al.* Structural changes in the gray matter of unmedicated patients with obsessive-compulsive disorder: a voxel-based morphometric study. Neurosci Bull 2013, 29: 642–648.

[22] Ishii K, Kawachi T, Sasaki H, Kono AK, Fukuda T, Kojima Y*, et al.* Voxel-based morphometric comparison between early- and late-onset mild Alzheimer's disease and assessment of diagnostic performance of z score images. AJNR Am J Neuroradiol 2005, 26: 333–340.

[23] Guo X, Wang Z, Li K, Li Z, Qi Z, Jin Z*, et al.* Voxel-based assessment of gray and white matter volumes in Alzheimer's disease. Neurosci Lett 2010, 468: 146–150.

[24] Hirata Y, Matsuda H, Nemoto K, Ohnishi T, Hirao K, Yamashita F*, et al.* Voxel-based morphometry to discriminate early Alzheimer's disease from controls. Neurosci Lett 2005, 382: 269–274.

[25] Matsuda H, Mizumura S, Nemoto K, Yamashita F, Imabayashi E, Sato N*, et al.* Automatic voxel-based morphometry of structural MRI by SPM8 plus diffeomorphic anatomic registration through exponentiated lie algebra improves the diagnosis of probable Alzheimer Disease. AJNR Am J Neuroradiol 2012, 33: 1109–1114.

[26] Lehmann M, Crutch SJ, Ridgway GR, Ridha BH, Barnes J, Warrington EK*, et al.* Cortical thickness and voxel-based morphometry in posterior cortical atrophy and typical Alzheimer's disease. Neurobiol Aging 2011, 32: 1466–1476.

[27] Shiino A, Watanabe T, Maeda K, Kotani E, Akiguchi I, Matsuda M. Four subgroups of Alzheimer's disease based on patterns of atrophy using VBM and a unique pattern for early onset disease. Neuroimage 2006, 33: 17–26.

[28] Canu E, Frisoni GB, Agosta F, Pievani M, Bonetti M, Filippi M. Early and late onset Alzheimer's disease patients have distinct patterns of white matter damage. Neurobiol Aging 2012, 33: 1023–1033.

[29] Liu Y, Yu C, Zhang X, Liu J, Duan Y, Alexander-Bloch AF*, et al.* Impaired Long Distance Functional Connectivity and Weighted Network Architecture in Alzheimer's Disease. Cereb Cortex 2013. doi: 10.1093/cercor/bhs410.

[30] Song J, Qin W, Liu Y, Duan Y, Liu J, He X*, et al.* Aberrant functional organization within and between resting-state networks in AD. PLoS One 2013, 8: e63727. doi: 10.1371/journal.pone.0063727.

[31] Mak HK, Zhang Z, Yau KK, Zhang L, Chan Q, Chu LW. Efficacy of voxel-based morphometry with DARTEL and standard registration as imaging biomarkers in Alzheimer's disease patients and cognitively normal older adults at 3.0 Tesla MR imaging. J Alzheimers Dis 2011, 23: 655–664.

[32] Yang J, Pan P, Song W, Huang R, Li J, Chen K*, et al.* Voxelwise meta-analysis of gray matter anomalies in Alzheimer's disease and mild cognitive impairment using anatomic likelihood estimation. J Neurol Sci 2012, 316: 21–29.

[33] Schroeter ML, Stein T, Maslowski N, Neumann J. Neural correlates of Alzheimer's disease and mild cognitive impairment: a systematic and quantitative meta-analysis involving 1351 patients. Neuroimage 2009, 47: 1196–1206.

[34] Zhang Z, Liu Y, Jiang T, Zhou B, An N, Dai H*, et al.* Altered

spontaneous activity in Alzheimer's disease and mild cognitive impairment revealed by Regional Homogeneity. Neuroimage 2012, 59: 1429–1440.

[35] Yao H, Liu Y, Zhou B, Zhang Z, An N, Wang P*, et al.* Decreased functional connectivity of the amygdala in Alzheimer's disease revealed by resting-state fMRI. Eur J Radiol 2013, 82: 1531–1538.

[36] Zhou B, Liu Y, Zhang Z, An N, Yao H, Wang P*, et al.* Impaired functional connectivity of the thalamus in alzheimer' s disease and mild cognitive impairment: a resting-state FMRI study. Curr Alzheimer Res 2013, 10: 754–766.

[37] Yesavage JA, Brink TL, Rose TL, Lum O, Huang V, Adey M*, et al.* Development and validation of a geriatric depression screening scale: a preliminary report. J Psychiatr Res 1982, 17: 37–49.

[38] Morris JC. The Clinical Dementia Rating (CDR): current version and scoring rules. Neurology 1993, 43: 2412–2414.

[39] Ledberg A, Akerman S, Roland PE. Estimation of the probabilities of 3D clusters in functional brain images. Neuroimage 1998, 8: 113–128.

[40] Poppenk J, Moscovitch M. A hippocampal marker of recollection memory ability among healthy young adults: contributions of posterior and anterior segments. Neuron 2011, 72: 931–937.

[41] Li S, Shi F, Pu F, Li X, Jiang T, Xie S*, et al.* Hippocampal shape analysis of Alzheimer disease based on machine learning methods. AJNR Am J Neuroradiol 2007, 28: 1339–1345.

[42] Shi F, Liu Y, Jiang T, Zhou Y, Zhu W, Jiang J*, et al.* Regional homogeneity and anatomical parcellation for fMRI image classification: application to schizophrenia and normal controls. Med Image Comput Comput Assist Interv 2007, 10: 136–143.

[43] Wang K, Jiang T, Liang M, Wang L, Tian L, Zhang X*, et al.* Discriminative analysis of early Alzheimer's disease based on two intrinsically anti-correlated networks with resting-state fMRI. Med Image Comput Comput Assist Interv 2006, 9: 340–347.

[44] Bishop CM. Pattern Recognition and Machine Learning. 1st ed: Springer-Verlag New York Inc, 2006: 179–220.

[45] Braak H, Braak E. Staging of Alzheimer's disease-related neurofibrillary changes. Neurobiol Aging 1995, 16: 271–278; discussion 278–284.

[46] Jin K, Peel AL, Mao XO, Xie L, Cottrell BA, Henshall DC*, et al.* Increased hippocampal neurogenesis in Alzheimer's disease. Proc Natl Acad Sci U S A 2004, 101: 343–347.

[47] Braak H, Braak E. Neuropathological stageing of Alzheimer-related changes. Acta Neuropathol 1991, 82: 239–259.

[48] Tombaugh TN, McIntyre NJ. The mini-mental state examination: a comprehensive review. J Am Geriatr Soc 1992, 40: 922–935.

[49] Petersen RC. Early diagnosis of Alzheimer's disease: is MCI too late? Curr Alzheimer Res 2009, 6: 324–330.

[50] Sperling RA, Aisen PS, Beckett LA, Bennett DA, Craft S, Fagan AM*, et al.* Toward defining the preclinical stages of Alzheimer's disease: recommendations from the National Institute on Aging-Alzheimer's Association workgroups on diagnostic guidelines for Alzheimer's disease. Alzheimers Dement 2011, 7: 280–292.

[51] Jack CR, Jr., Albert MS, Knopman DS, McKhann GM, Sperling RA, Carrillo MC*, et al.* Introduction to the recommendations from the National Institute on Aging-Alzheimer's Association workgroups on diagnostic guidelines for Alzheimer's disease. Alzheimers Dement 2011, 7: 257–262.

[52] McKhann GM, Knopman DS, Chertkow H, Hyman BT, Jack CR, Jr., Kawas CH*, et al.* The diagnosis of dementia due to Alzheimer's disease: recommendations from the National Institute on Aging-Alzheimer's Association workgroups on diagnostic guidelines for Alzheimer's disease. Alzheimers Dement 2011, 7: 263–269.

[53] Shen Q, Loewenstein DA, Potter E, Zhao W, Appel J, Greig MT*, et al.* Volumetric and visual rating of magnetic resonance imaging scans in the diagnosis of amnestic mild cognitive impairment and Alzheimer's disease. Alzheimers Dement 2011, 7: e101–108.

[54] Diniz BS, Nunes PV, Yassuda MS, Forlenza OV. Diagnosis of mild cognitive impairment revisited after one year. Preliminary results of a prospective study. Dement Geriatr Cogn Disord 2009, 27: 224–231.

[55] Petersen RC. Mild cognitive impairment clinical trials. Nat Rev Drug Discov 2003, 2: 646–653.

[56] Busse A, Hensel A, Guhne U, Angermeyer MC, Riedel-Heller SG. Mild cognitive impairment: long-term course of four clinical subtypes. Neurology 2006, 67: 2176–2185.

[57] Holtzman DM, Morris JC, Goate AM. Alzheimer's disease: the challenge of the second century. Sci Transl Med 2011, 3: 77sr71.

[58] Augustinack JC, Magnain C, Reuter M, van der Kouwe AJ, Boas D, Fischl B. MRI parcellation of *ex vivo* medial temporal lobe. Neuroimage 2013. doi: 10.1016/j.neuroimage.2013.05.053.

[59] Amunts K, Kedo O, Kindler M, Pieperhoff P, Mohlberg H,

Shah NJ*, et al.* Cytoarchitectonic mapping of the human amygdala, hippocampal region and entorhinal cortex: intersubject variability and probability maps. Anat Embryol (Berl) 2005, 210: 343–352.

[60] Toga AW. The clinical value of large neuroimaging data sets in Alzheimer's disease. Neuroimaging Clin N Am 2012, 22: 107–118, ix.

[61] Busatto GF, Diniz BS, Zanetti MV. Voxel-based morphometry in Alzheimer's disease. Expert Rev Neurother 2008, 8: 1691–1702.

[62] Ridgway GR, Henley SM, Rohrer JD, Scahill RI, Warren JD, Fox NC. Ten simple rules for reporting voxel-based morphometry studies. Neuroimage 2008, 40: 1429–1435.

[63] Ceccarelli A, Jackson JS, Tauhid S, Arora A, Gorky J, Dell'Oglio E*, et al.* The impact of lesion in-painting and registration methods on voxel-based morphometry in detecting regional cerebral gray matter atrophy in multiple sclerosis. AJNR Am J Neuroradiol 2012, 33: 1579–1585.

[64] Duda RO, Hart PE, Stork DG. Pattern Classification. New York: John Wiley Sons, 2001: 184–221.